Chapter 10

Magnetocaloric and Magnetic Properties of Meta-Magnetic Heusler Alloy $Ni_{41}Co_9Mn_{31.5}Ga_{18.5}$

Takuo Sakon, Takuya Kitaoka, Kazuki Tanaka,
Keisuke Nakagawa, Hiroyuki Nojiri,
Yoshiya Adachi and Takeshi Kanomata

Additional information is available at the end of the chapter

http://dx.doi.org/10.5772/64375

Abstract

$Ni_{41}Co_9Mn_{31.5}Ga_{18.5}$ is a magnetic Heusler alloy, which indicates metamagnetic transition at the reverse martensite transition. In this paper, caloric measurements were performed and discussed about magnetocaloric effect. We also performed magnetization measurements around Curie temperature T_C in the martensite phase and analyzed by means of the spin fluctuation theory of itinerant electron magnetism. From the differential scanning calorimetry (DSC) measurements in zero fields, the value of the latent heat λ was obtained as 2.63 kJ/kg, and in magnetic fields the value was not changed. The entropy change ΔS was − 7.0 J/(kgK) in zero fields and gradually increases with increasing magnetic fields. The relative cooling power (RCP) was 104 J/kg at 2.0 T, which was comparable with In doped $Ni_{41}Co_9Mn_{32}Ga_{16}In_2$ alloy.

The results of magnetization measurement were in agreement with the theory of Takahashi, concerning itinerant electron magnetism. From the M^4 vs H/M plot, the spin fluctuation temperature T_A can be obtained. The obtained T_A was 703 K and which was smaller than Ni (1.76×10^4 K). The value was comparable to that of UGe_2 (493 K), which is famous for the strongly correlated heavy fermion ferromagnet.

Keywords: shape memory alloys, differential scanning calorimetry, magnetocaloric effect, magnetization, itinerant electron magnetism

1. Introduction

Recently, ferromagnetic shape memory alloys (FSMA) have been studied extensively as candidates for highly functional materials. Between FSMA, Ni_2MnGa is the most renowned alloy [1]. The alloy has a cubic $L2_1$ Heusler structure, with a space group of $\boldsymbol{Fm\bar{3}m}$, and ferromagnetic transition occurs at the Curie temperature, T_C, 365 K [2, 3]. Cooling from ordinary temperature, a martensite transition occurs at the martensite transition temperature, T_M, 200 K. Below T_M, a superstructure state is realized as a result of lattice modulation [4, 5]. For Ni_2MnGa type alloys, $\boldsymbol{T_M}$**'s** are varied from 200 to 330 K by non-stoichiometrically varying the concentration of constituent elements of the alloys. Sakon et al. studied about the magnetic properties of $\mathbf{Ni_{50+x}Mn_{27-x}Ga_{23}}$ [6]. The martensite transition and the ferromagnetic transition occurred at the same temperature at the martensite transition temperature T_M for x = 2.5, 2.7. The T_M shift in magnetic fields around a zero magnetic field was estimated to be dT_M/dB = 1.1 ± 0.2 K/T, thus indicating that magnetization influences martensite transition.

New alloys in the Ni–Mn–In, Ni–Mn–Sn, and Ni–Mn–Sb Heusler alloy systems that are expected to be ferromagnetic shape memory alloys have been studied [7, 8]. A metamagnetic transition from paramagnetic martensite phase to ferromagnetic austenite phase was observed, and reverse martensite transition induced by magnetic fields was occurred under high magnetic fields [9, 10]. These alloys are promising as a metamagnetic shape memory alloys with a magnetic field-induced shape memory effect (MSIF) and as magnetocaloric materials. Ni–Co–Mn–In alloys, in which Co is substituted for Ni in Ni–Mn–In alloys to increase the Curie temperature, indicate shape memory behaviors in compressive **stress–strain** measurements. It is noticeable that 3% MFIS has been observed for $Ni_{45}Co_5Mn_{36.7}In_{13.3}$ [11].

The substitution of Co for Ni or Ga atoms in Ni_2MnGa type alloys has turned the magnetic ordering of the parent phase from partially antiferromagnetic or paramagnetic to ferromagnetic, resulting in a large magnetization change across the transformation, which dramatically enhances the magnetic field driving force [12–40]. The phase diagram in the temperature-concentration plane is determined on the basis of the experimental results. The determined phase diagram is spanned by a paramagnetic austenite (Para-A) phase, paramagnetic martensite phase, ferromagnetic austenite phase, ferromagnetic martensite (Ferro-M) phase of $\mathbf{Ni_{50-x}Co_xMn_{31.5}Ga_{18.5}}$ [41]. The measurements indicated that a magnetostructural transition between the Para-A and Ferro-M phases. As for $Ni_2MnGa_{1-x}Co_x$ ($0 \le x \le 0.20$), which was substituted of Co for Ga, the measurements showed that a magnetostructural transition between the Para-A and Ferro-M phases does not appear in this alloy system [21]. Therefore, the experimental studies of the Ni_2MnGa type Heusler compounds, which were substituted of Co for Ni atoms, are important to clarify the nature of the magnetostructural interactions, which is one of the important problems in the physics of Heusler compounds. The transformation temperature can be downshifted by magnetic field at a rate $\boldsymbol{dT_R/\mu_0 dH}$ or $\boldsymbol{dT_M/\mu_0 dH}$ up to 14 K/T in $Ni_{37}Co_{13}Mn_{32}Ga_{18}$ [39]. The aging effect is also important. Segui et al. measured the thermo-magnetization, M-T, of $Ni_{43}Co_7Mn_{32}Ga_{18}$ at the constant magnetic fields of **5** mT [13, 15, 42]. As longer aging time, the larger value of the magnetization was obtained at ferromagnetic austenite phase around 420 K. This indicates that the improvement of atomic

http://dx.doi.org/10.5772/64375

order enhances the ferromagnetic character. Castillo-Villa et al. reported about the elastocaloric effect in a $Ni_{50}Mn_{25-x}Ga_{25}Co_x$ [25]. They also studied the influence of applied magnetic fields on this effect experimentally, and a comparative investigation with the magnetocaloric effect, which was exhibited by the alloy, was performed. Both of the elastocaloric and magnetocaloric effects are a result of the martensite transition incurred by the alloy. The influence of a compressive stress and of a magnetic field is to gain the stability of the martensite phase. It leads to an increase of the transition temperature with applied stress and magnetic field. The magnetic properties of $Ni_{33.0}Co_{13.4}Mn_{39.7}Ga_{13.9}$ were investigated by Xu *et al.* [28]. It is noticeable that the kinetic arrest phenomenon was observed at about 120 K by thermomagnetization measurements. Magnetic field-induced transformation was also detected at the temperatures between 4.2 and 300 K. In this phenomenon, martensite transition is interrupted at certain temperatures (kinetic arrest temperature, T_{KA}) during field cooling and does not proceed with further cooling. It was confirmed that the transformation entropy change below 120 K becomes almost zero, which results in the kinetic arrest phenomenon by evaluation of the equilibrium magnetic fields and temperatures based on the transformation fields and temperatures.

Albertini *et al.* has been performed experimental studies about the composition dependence of the structural and magnetic properties of the Ni–Mn–Ga ferromagnetic shape memory alloy substituted of Co for Ni atoms around the composition of $Ni_{50}Mn_{30}Ga_{20}$ [12, 31]. The magnetic and structural properties displayed remarkable discontinuities across the martensite transition. There was a clear jump (ΔM) in the saturation magnetization at the transformation, which indicates that a metamagnetic transition appeared in the magnetic field. The field dependence of the martensite transition temperature, $dT_M/\mu_0 dH$, and that of the crystalline volume change, $\Delta V/V$, was reported. The most notable alloy is $Ni_{41}Co_9Mn_{32}Ga_{18}$. When cooling from 500 K, a ferromagnetic transition in the austenite phase at T_C^A = 456 K. At the martensite transition temperature, T_M = 420 K, the AC susceptibility decreased drastically. Below 300 K, the AC susceptibility gradually increased and a distinct peak was found at the Curie temperature T_C^M = 257 K in the martensite phase. Heating from 200 K, the Curie temperatures T_C^M and T_C^A were just the same with the temperatures in the cooling procedure. The reverse martensite temperature T_R was 436 K. Therefore, the AC susceptibility indicates re-entrant magnetism, ferromagnetic-paramagnetic state, which should be released to the crystal structures. The $dT_M/\mu_0 dH$ and $\Delta V/V$ were found to be considerably enhanced by the additional in-doping of the **Ni–Co–Mn–Ga** alloy [12]. The entropy change is larger than that of **Ni–Co–Mn–Ga,** which suggests large relative cooling power (RCP).

We studied about the physical properties and magnetism of $Ni_{50-x}Co_xMn_{31.5}Ga_{18.5}$ [41]. Crystallographic, thermal strain, and magnetic properties of $Ni_{50-x}Co_xMn_{38.5}Ga_{18.5}$ ($0 \le x \le 9$) were investigated across the martensite transition temperature T_M and the reverse martensite transition temperature T_R at atmospheric pressure above T_C^M = 263 K. These transition temperatures increased gradually with increasing Co component x. Moreover, temperature hysteresis in the thermal cycles of the magnetization across the T_R and T_M, became larger with increasing x. As for x = 9, $Ni_{41}Co_9Mn_{31.5}Ga_{18.5}$, extensive temperature hysteresis of $T_M - T_R$ = 65 K was found in the thermal strain measurement. The metamagnetic transition was observed

from the paramagnetic martensite phase to the ferromagnetic austenite phase between 330 and 390 K. Under atmospheric pressure, the observed magnetostriction value of this alloy at 350 K was 0.11%. This value is larger than that of Tb-Dy-Fe single crystal [43]. In this study, $Ni_{50-x}Co_xMn_{38.5}Ga_{18.5}$ was polycrystal, and it is easy for processing and handling. Moreover, the magnetostriction effect occurred at a temperature between room temperature and 400 K, which was suggested that it is useful in the high temperature region, *for example,* apparatus in the engine room of the motorcar.

The effects of Co addition on the properties of $Ni_{8-x}Mn_4Ga_4Co_x$ ($x = 0, 1, 2$) ferromagnetic shape memory alloys are systematically investigated by first-principles calculations by Bai et al. [26]. The results of formation energy indicate that the added Co preferentially occupies the Ni sites in Ni_2MnGa alloy. The total energy difference between the paramagnetic and the ferromagnetic austenite plays an important role on the Curie transformation. Increasing Co content, electron density of states, DOS, of down spins around the Fermi level gradually decreases. On the contrary, those of the up spin almost remain without changing. This causes enhancement of the magnetic moments in these alloys. This result indicates that the investigation of the itinerant electron magnetism is important to understand the physics and magnetism of these alloys more deeply.

In this paper, caloric measurements were performed. On the basis of the experimental results, magnetocaloric effect was discussed. We also studied about the itinerant electron magnetic properties of $Ni_{41}Co_9Mn_{31.5}Ga_{18.5}$. We performed the magnetization measurements by means of the pulsed magnetic fields. The M^4 vs H/M plot crossed the coordinate axis at the Curie temperature in the martensite phase, T_C^M, and the plot indicates a good linear relation behavior around the T_C^M. The magnetization results were analyzed by means of the theory of Takahashi, concerning itinerant electron magnetism [44, 45] and the spin fluctuation temperature T_A can be obtained. We discussed about the itinerant magnetism of $Ni_{41}Co_9Mn_{31.5}Ga_{18.5}$ by means of the magnetization measurements.

2. Experimental procedures

The sample used in this study was synthesized at Yamagata University. The $Ni_{41}Co_9Mn_{31.5}Ga_{18.5}$ alloy was prepared by arc melting 4N Ni, 4N Co, 4N Mn, and 6N Ga in an argon atmosphere. The sample annealed at 1123 K for three days to homogenize the sample in a double evacuated silica tube, and then quenched in cold water. The obtained sample was polycrystalline. DSC measurements were performed by means of Helium-free magnet at High Field Laboratory for Superconducting Materials, Institute for Materials Research, Tohoku University. The bore of this magnet is 100 mmϕ in the air and which installed the factory-made DSC equipment.

Magnetization measurements were performed by means of the pulsed field magnet at Ryukoku University. The absolute value was adjusted by Ni. The diamagnetism of the sample was also concerned to analyze the field dependence of the magnetization.

http://dx.doi.org/10.5772/64375

3. Results and discussions

3.1. Crystallography of $Ni_{41}Co_9Mn_{31.5}Ga_{18.5}$

From X-ray powder diffraction shown in **Figure 1**, the sample was confirmed as a single phase with a tetragonal $D0_{22}$ structure at 298 K, as shown in **Figure 2**. The lattice parameters of the tetragonal structure were $a = 3.8794$ Å and $c = 6.6247$ Å. The size of the sample was 0.8 mm × 3.0 mm × 4.0 mm.

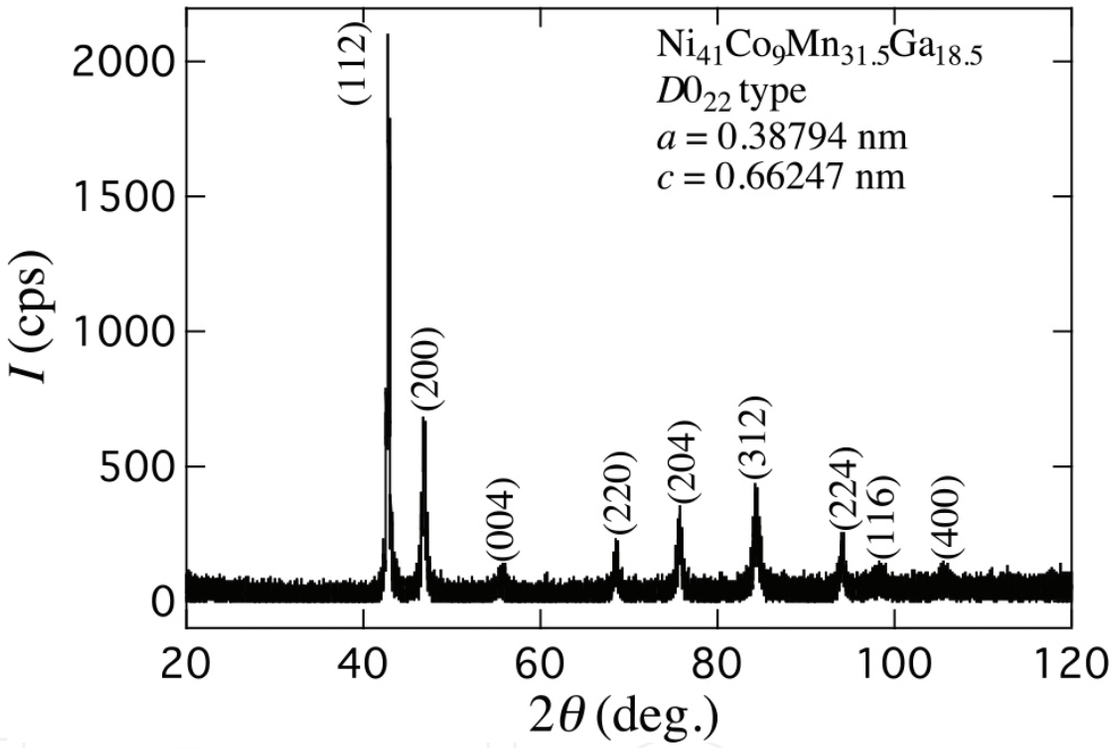

Figure 1. X-ray powder diffraction pattern of $Ni_{41}Co_9Mn_{31.5}Ga_{18.5}$ at 298 K, which indicates $D0_{22}$ type martensite phase.

The final compositions of the grown sample were verified by energy dispersive spectroscopy and were close to the nominal values with a deviation of <1%.

The Scanning Electron Microscope (SEM) image of $Ni_{41}Co_9Mn_{31.5}Ga_{18.5}$ at 298 K by means of FE-SEM (JSM6300F, JEOL Co. Ltd.) shown in **Figure 3** indicates that there are macroscopic twin variants on a scale of a few micrometers. The twins were arranged neatly in the domains. A single martensite phase characterized by typical lamellar twin substructures was observed, agreeing well with the X-ray diffraction results. This result is well agree with the optical micrographs of microstructure of $Ni_{56-x}Co_xMn_{25}Ga_{19}$ ($x = 2, 4, 8$) [32].

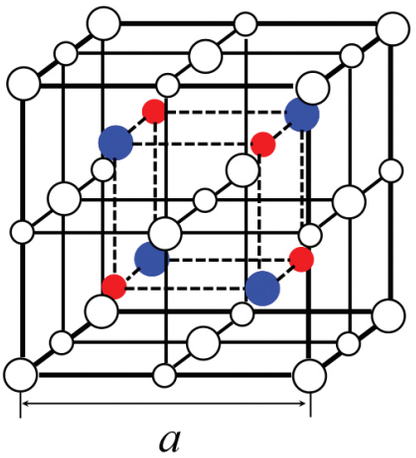

Austenite phase. Cubic $L2_1$ Heusler structure.

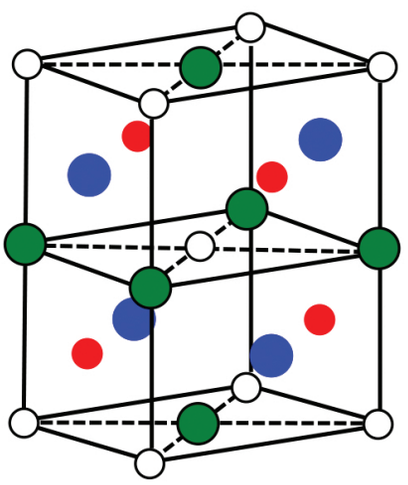

Al_3Ti ($D0_{22}$-type)

Martensite phase. $D0_{22}$ structure.

Figure 2. Schematic drawings of crystal structures in austenite phase and martensite phase.

http://dx.doi.org/10.5772/64375

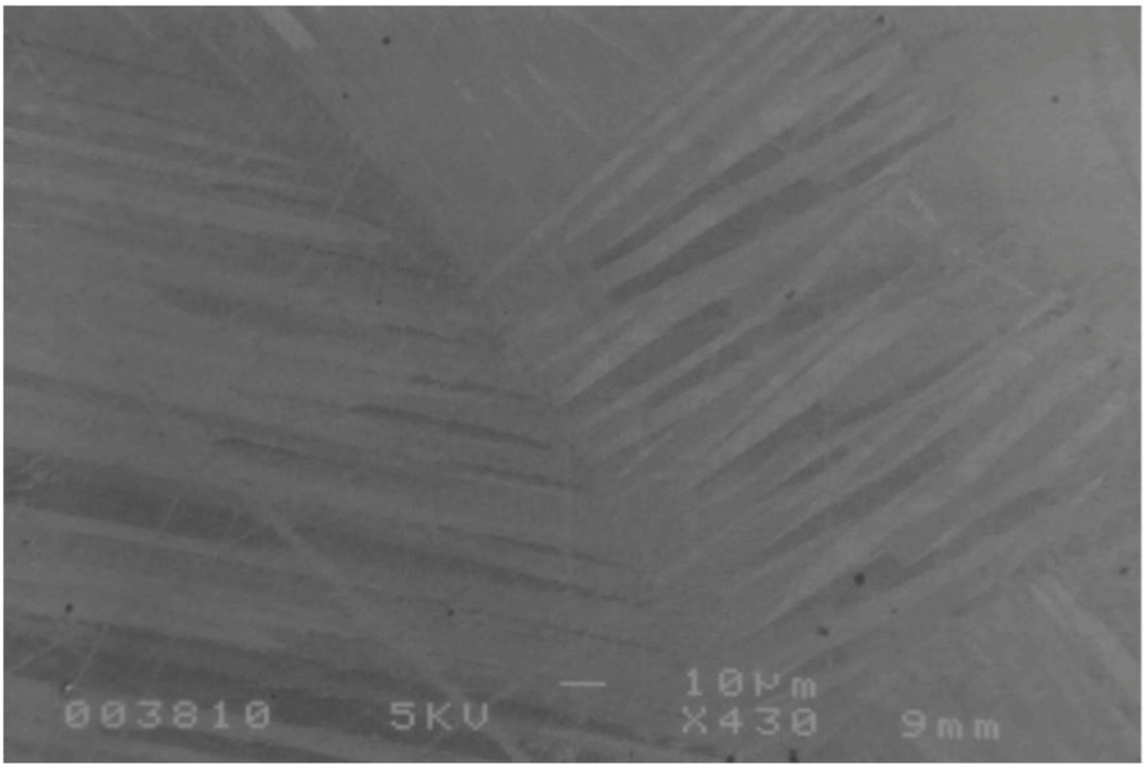

Figure 3. Scanning electron microscope i_m age of $Ni_{41}Co_9Mn_{31.5}Ga_{18.5}$ at 298 K by means of FE-SEM.

The calorimetric measurements, which allowed for the estimation of the latent heat and magnetocaloric analysis, were performed with factory-made differential scanning calorimeter able to work up to 6 T. This setup exploits Peltier cells in order to measure heat flow of the sample. Calorimetric measurements of $Ni_{41}Co_9Mn_{31.5}Ga_{18.5}$ polycrystalline ferromagnetic shape memory alloy (FSMA) were performed across the T_R. As for the reference value of the latent heat λ at zero magnetic fields, calorimetric measurements were performed by the commercial DSC system, DSC3300 (Materials Analysis and Characterization Co., Ltd.). The measured value of the λ at zero fields was 2.63 kJ/kg around $T_R = 380$ K.

3.2. Magnetocaloric effect of $Ni_{41}Co_9Mn_{31.5}Ga_{18.5}$

The thermodynamic properties of the presented sample in magnetic fields were studied experimentally by measuring the heat flow by means of the DSC equipment. The four panels of **Figure 4** show the heat flow of $Ni_{41}Co_9Mn_{31.5}Ga_{18.5}$ in zero and magnetic fields. The endothermic reaction was occurred around the reverse martensite temperature T_R. These calorimetry experiments confirm the values of the ratio of field change of the transition temperature $dT_R/\mu_0 dH$ deduced from thermal expansion measurements [46]. The latent heat λ of the fully transformed reverse martensite transition, as shown in the four panels of **Figure 5** was calculated by integrating the heat flow profile in **Figure 4** for each magnetic field. The entropy S was calculated as $S = \lambda/T$. The entropy of $Ni_{41}Co_9Mn_{31.5}Ga_{18.5}$ at 0 and 2 T are shown in **Figure 6**.

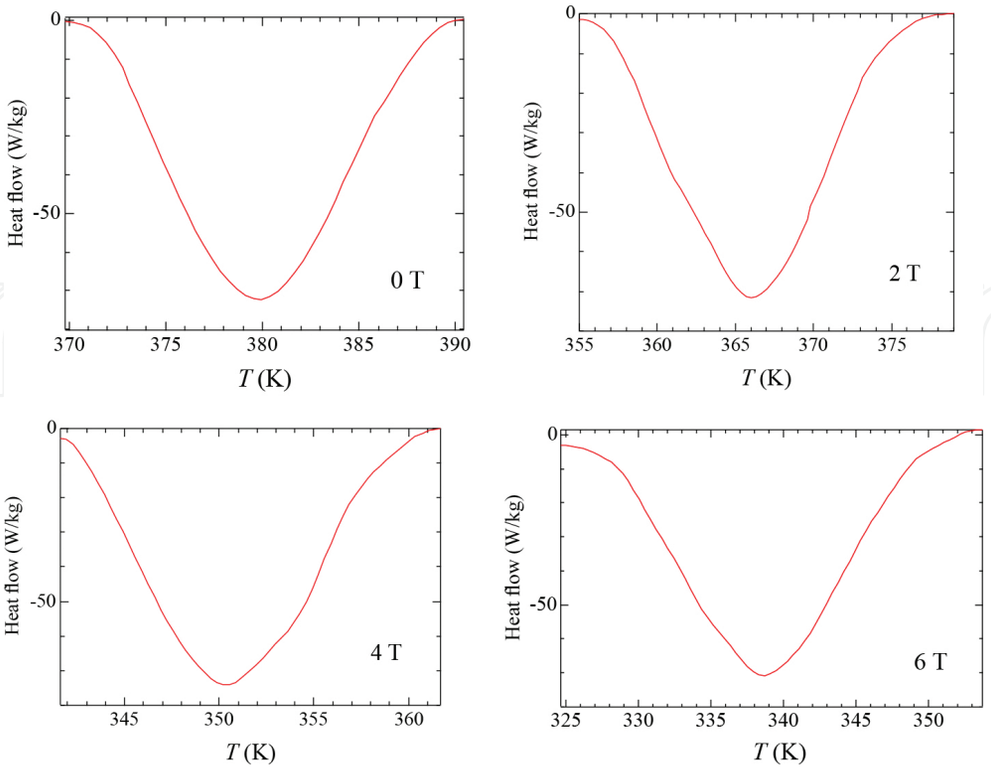

Figure 4. Heat flow of $Ni_{41}Co_9Mn_{31.5}Ga_{18.5}$ in zero and magnetic fields.

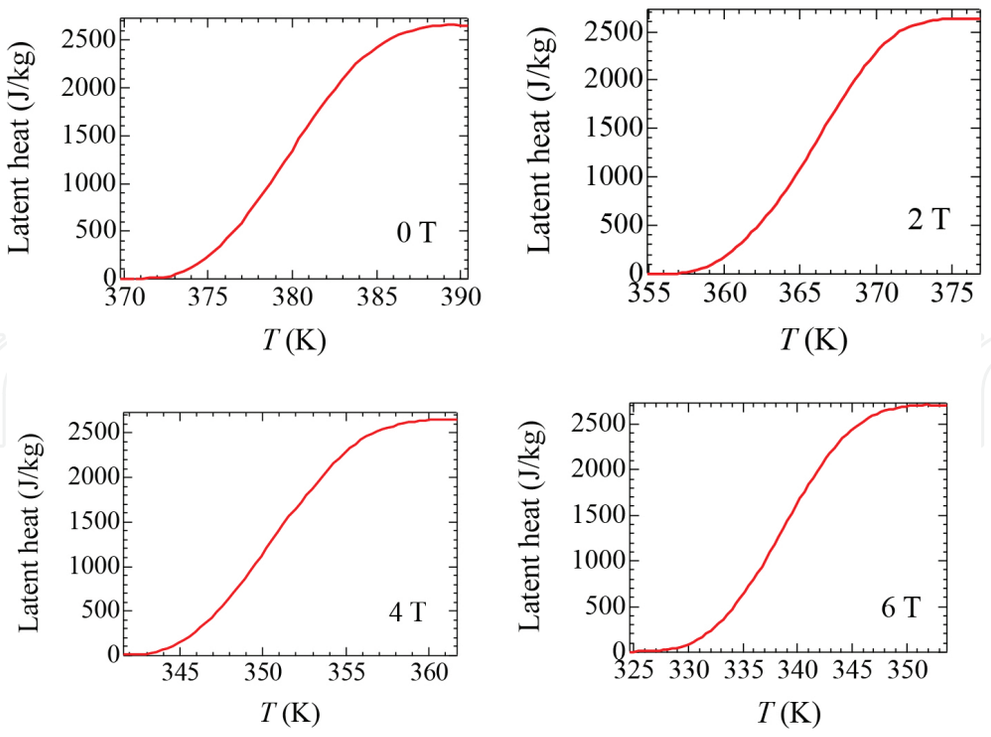

Figure 5. Latent heat of $Ni_{41}Co_9Mn_{31.5}Ga_{18.5}$ in zero and magnetic fields.

http://dx.doi.org/10.5772/64375

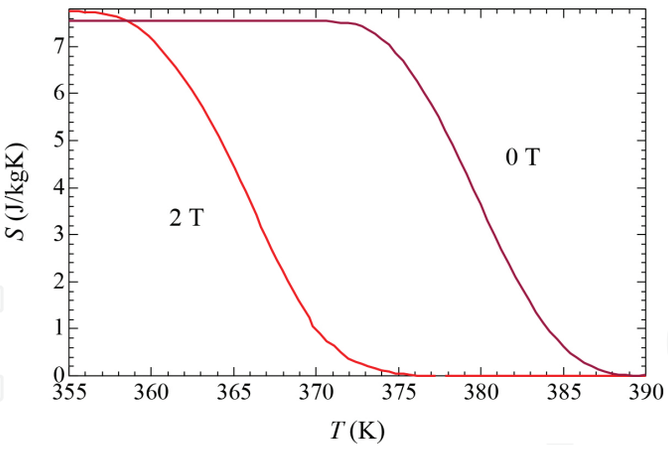

Figure 6. Entropy of $Ni_{41}Co_9Mn_{31.5}Ga_{18.5}$ at 0 and 2 T.

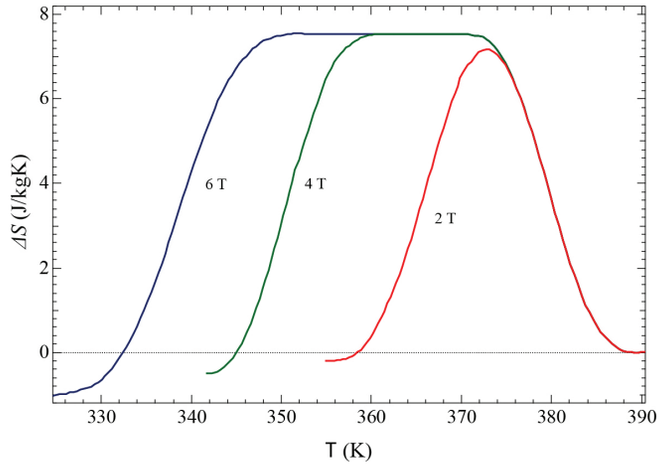

Figure 7. Entropy change ΔS of $Ni_{41}Co_9Mn_{31.5}Ga_{18.5}$.

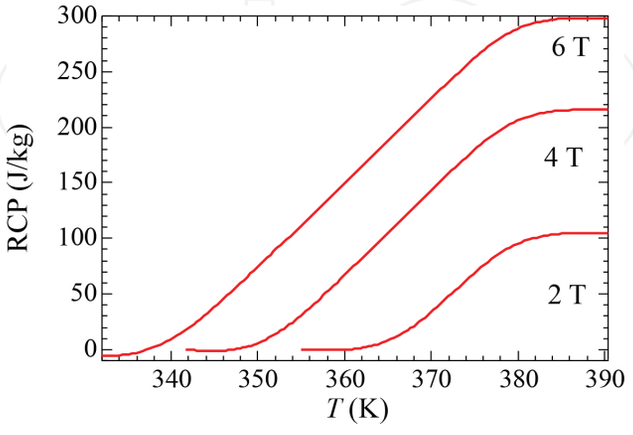

Figure 8. Relative cooling power of $Ni_{41}Co_9Mn_{31.5}Ga_{18.5}$.

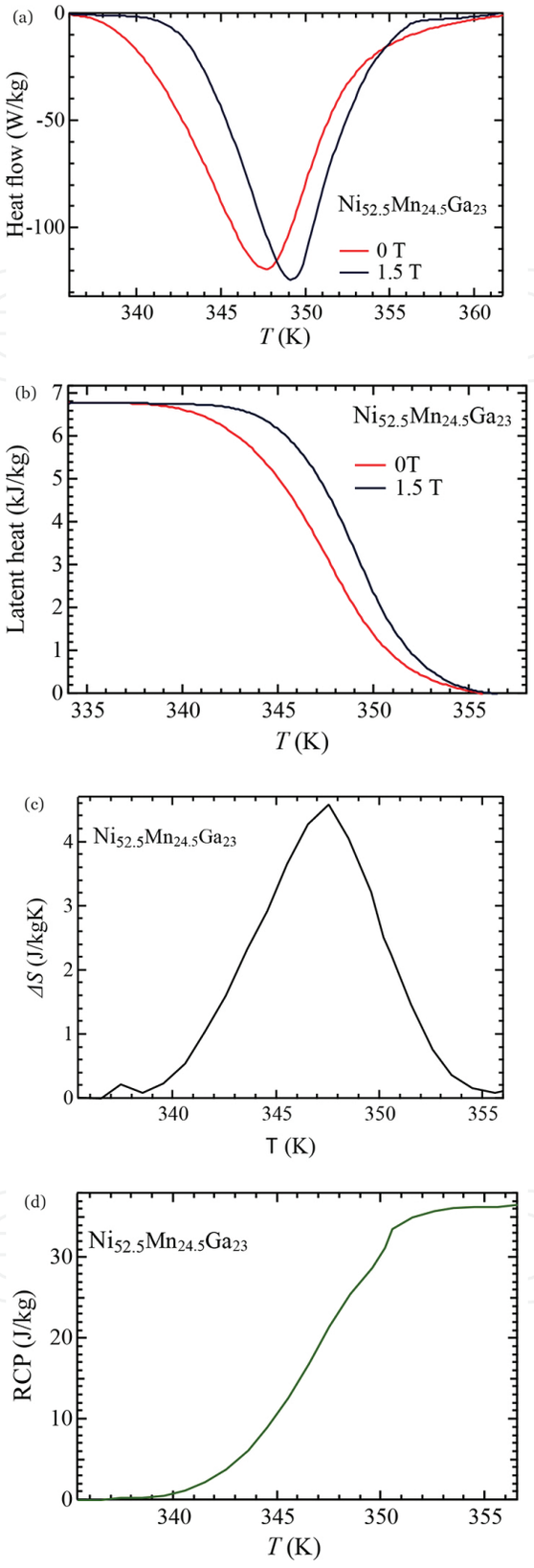

Figure 9. (a) Heat flow of $Ni_{52.5}Mn_{24.5}Ga_{23}$; (b) latent heat of $Ni_{52.5}Mn_{24.5}Ga_{23}$; (c) ΔS of $Ni_{52.5}Mn_{24.5}Ga_{23}$; and (d) RCP of $Ni_{52.5}Mn_{24.5}Ga_{23}$.

http://dx.doi.org/10.5772/64375

Figure 7 shows the entropy change $\Delta S = S(\mu_0 H) - S(0)$ of $Ni_{41}Co_9Mn_{31.5}Ga_{18.5}$. The relative cooling power (RCP) was calculated by integrating the ΔS in the temperature, as shown in **Figure 8**. The calculated RCP was 104 J/kg at 2.0 T, which was comparable with $Ni_{50}Mn_{35}In_{14}Si_1$ and $Ni_{41}Co_9Mn_{32}Ga_{16}In_2$ alloy [47].

We also performed the DSC measurement of $Ni_{52.5}Mn_{24.5}Ga_{23}$ in zero and magnetic fields by means of the water-cooled electromagnet in Ryukoku University. **Figure 9a** shows the heat flow of $Ni_{52.5}Mn_{24.5}Ga_{23}$ in a heating process. The endothermic reaction was occurred around $T_R = 348$ K. In the external magnetic field of 1.5 T, the reaction was also occurred. The $dT_R/\mu_0 dH$ obtained from DSC measurements in **Figure 9a** were 1.1 K/T, which is comparable to the results of the thermal strain measurements [6]. **Figure 9b** shows the latent heat λ of $Ni_{52.5}Mn_{24.5}Ga_{23}$. The λ is larger than that of $Ni_{41}Co_9Mn_{31.5}Ga_{18.5}$. **Figure 9c** shows the entropy change ΔS of $Ni_{52.5}Mn_{24.5}Ga_{23}$. The value was 4.6 J/kg K, which is comparable to the value of $Ni_{52.6}Mn_{23.1}Ga_{24.3}$ [48]. **Figure 9d** shows the RCP of $Ni_{52.5}Mn_{24.5}Ga_{23}$. The value was 36 J/kg.

Table 1 shows the T_M, ΔS, δT, and RCP at 2 T. δT indicates the half width of the ΔS. The ΔS, δT, and RCP of $Ni_{52.5}Mn_{24.5}Ga_{23}$ were estimated from the DSC result at zero field and 1.5 T in this study. The three alloys of the beginning cause martensite phase transition at temperature of the T_M in paramagnetic austenite from ferromagnetic martensite. Four last alloys cause re-entrant magnetism at the temperature of T_M. The $dT_M/\mu_0 dH$ of the four last alloys is larger than that of the three alloys of the beginning. Therefore, the RCP is relatively larger than former alloys.

Sample	T_M (K)	ΔS (J/kg K)	δT (K)	RCP (J/kg)	Reference
$Ni_{52.6}Mn_{23.1}Ga_{24.3}$	297	-6	1.8	11	[48]
$Ni_{52.5}Mn_{24.5}Ga_{23}$	348	-6.1	8.0	48	This work
$Ni_{55.4}Mn_{20}Ga_{24.6}$	313	-41	1.1	45	[49]
$Ni_{45}Co_5Mn_{38}Sb_{12}$	264	26	2.8	73	[50]
$Ni_{50}Mn_{35}In_{14}Si_1$	288	36	2.6	94	[51]
$Ni_{43}Co_7Mn_{31}Ga_{19}$	420 (T_R 433)	13.3 (5 T)	–	188 (5 T)	[24]
$Ni_{41}Co_9Mn_{32}Ga_{18}$	421 (T_R 456)	17.8 (5 T)	12 (5 T)	156 (5 T)	[24]
$Ni_{45}Co_5Mn_{37.5}In_{12.5}$	355	7	16	112	[52]
$Ni_{41}Co_9Mn_{31.5}Ga_{18.5}$	348 (T_R 380)	7.2	14	104	This work

Table 1. The martensite transition temperature T_M, the maximum value of the entropy change ΔS, the half width of the entropy change δT, and the relative cooling power (RCP) at 2 T.

The magnetostructural transformation in this system can be described, in the frame of a simple geometrical model, by a relation linking the field-induced adiabatic temperature change ΔT_{ad} with $dT_M/\mu_0 dH$, with the martensite specific heat value $C_p^{Mart} = 490$ J/kg K, which was obtained by means of DSC in zero fields, the transformation temperature T_M and the entropy change ΔS [47], as the formula of,

$$\Delta T_{ad} = \frac{\Delta S \cdot \Delta T_M}{\Delta S + \Delta T_M \cdot \frac{C_p^{Mart}}{T_M}} \quad (1)$$

Here, $\Delta T_M = (dT_M/\mu_0 dH) \cdot \mu_0 \Delta H$ is the effective transformation shift in temperature induced by a magnetic field variation $\mu_0 \Delta H$. Fabbrici et al. commented about the relation between ΔT_{ad} and $dT_M/\mu_0 dH$. Eq. (1) provides important information about the relation between ΔT_{ad}, $dT_M/\mu_0 dH$ and ΔS. ΔT_{ad} is not instantaneously proportional either to $dT_M/\mu_0 dH$ or ΔS. This is a immediate consequence of the fact that the minute relation $\Delta T_{ad} = (T_M/C_p^{Mart})\ \Delta S$ cannot be directly extrapolated to finite differences. This is because that the specific heat, $C_p(H, T)$ depends on magnetic field and the temperature.

In order to obtain an adiabatic temperature change ΔT_{ad} from the results of the thermal measurements, the model proposed by Procari et al. is used [19, 53]. In **Figure 11**, the gradient of the entropy curve between AC in zero fields is equal to $C_p/T = 1.5 \pm 0.1$ J/kg K^2 is considered, where C_p is the specific heat. According to Porcali's model, the ΔT_{ad} is obtained as −4.5 K, which was shown in an arrow. The error between the calculated value $\Delta T_{ad} = -3.2$ K from Eq. (1) and experimentally obtained value $\Delta T_{ad} = -4.5$ K from **Figure 10** is 30%. It is correct qualitatively. **Table 2** shows the adiabatic temperature change of the Heusler alloys. The absolute value of ΔT_{ad} of the alloys, which shows re-entrant magnetism and metamagnetism is larger than that of the alloys which shows the magnetostructural transition from martensite ferromagnet to austenite paramagnet. This result is due to the large $dT_M/\mu_0 dH$ value of $Ni_{41}Co_9Mn_{32}Ga_{16}In_2$ and $Ni_{41}Co_9Mn_{31.5}Ga_{18.5}$. Consequently, large MCE has been appeared in $Ni_{41}Co_9Mn_{31.5}Ga_{18.5}$.

Entel et al. studied about $Ni_{50-x}Co_xMn_{39}Sn_{11}$ for $0 \le x \le 10$ [16]. The experimental phase diagram of $Ni_{50-x}Co_xMn_{39}Sn_{11}$ resembles that of $Ni_{50-x}Co_xMn_{31.5}Ga_{18.5}$ [41]. The T_M of $Ni_{50-x}Co_xMn_{31.5}Ga_{18.5}$ gradually decreases with increasing content x and temperature above $x = 9$, T_M drastically decreases. The T_M of $Ni_{50-x}Co_xMn_{39}Sn_{11}$ also shows same x dependence. Around $x = 8.5$, T_M drastically decreases. Entel et al. also suggested that superparamagnetic behavior or superspin glass phase has been appeared in martensite phase. As observed for some nonmagnetic martensitic systems, disorder and local structural distortions can lead to strain glass in austenite. Wang et al. reported that both a strain glass transition and a ferromagnetic transition take place in a $Ni_{55-x}Co_xMn_{20}Ga_{25}$ Heusler alloys [22], which results in a ferromagnetic strain glass with coexisting short-range strain ordering and long-range magnetic moment ordering for $10 \le x \le 18$. As for $Ni_{50-x}Co_xMn_{31.5}Ga_{18.5}$, microscopic (X-ray diffraction, neutron diffraction, μSR, etc.), measurements should be needed to clarify these problems. The complex magnetic and structural properties of Co-doped Ni–Mn–Ga Heusler alloys have been investigated by using a combination of first-principles calculations and classical Monte Carlo simulations by Sokolovskiy et al. [54]. The Monte Carlo simulations with *ab initio* exchange coupling constants as input parameters allow one to discuss the behavior at finite temperatures and to determine magnetic transition temperatures. The simulated magnetic and magnetocaloric properties of Co- and in-doped Ni-Mn-Ga alloys were in good qualitative agreement with the available experimental data. A similar calculation is expected in $Ni_{50-x}Co_xMn_{31.5}Ga_{18.5}$.

http://dx.doi.org/10.5772/64375

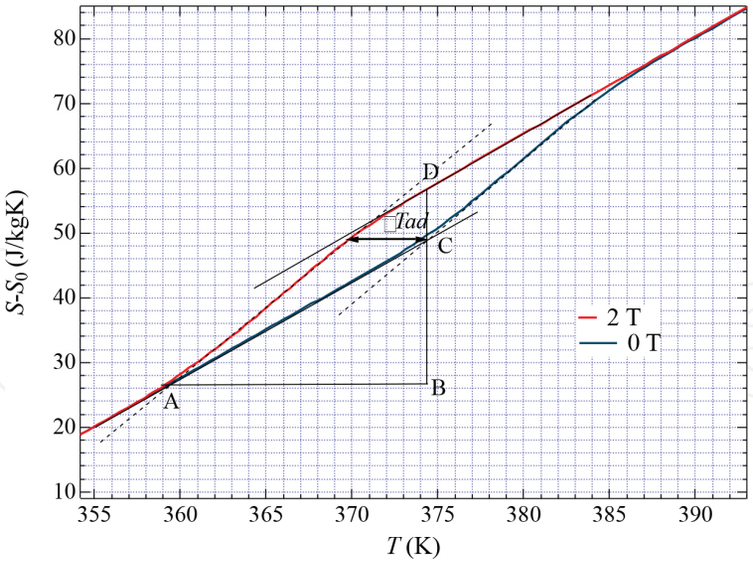

Figure 10. Real heating calorimetric $S(T, H)$ curves across the reverse martensite transition of $Ni_{41}Co_9Mn_{31.5}Ga_{18.5}$. The geometrical construction has superimposed on them.

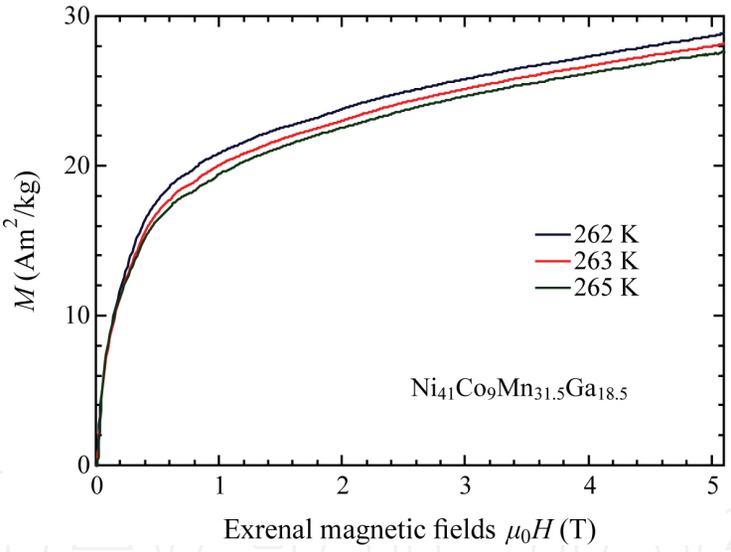

Figure 11. Magnetization process of $Ni_{41}Co_9Mn_{31.5}Ga_{18.5}$.

Sample	λ (kJ/kg)	ΔS (J/kg K)	ΔT_M (K)	T_M (K)	ΔT_{ad} (μ_0 H[T]) (K)	Reference
$Ni_{50}Mn_{30}Ga_{20}$	6.90	-3.7	+0.9	370	+0.8 (1.8 T)	[47]
$Ni_{52.5}Mn_{24.5}Ga_{23}$	6.78	-4.6	+1.5	348	+1.0 (1.5 T)	This work
$Ni_{41}Co_9Mn_{32}Ga_{16}In_2$	2.30	4.5	-11.3	320	-2.3 (1.8 T)	[42, 47]
$Ni_{41}Co_9Mn_{31.5}Ga_{18.5}$	2.34	7.2	-8.6	348	-4.5 (2.0 T)	This work

Table 2. The adiabatic temperature change of the Heusler alloys.

3.3. Itinerant electron magnetic properties of $Ni_{41}Co_9Mn_{31.5}Ga_{18.5}$

We performed the magnetization measurements by means of the pulsed magnetic fields in order to investigate the itinerant electron magnetic properties of $Ni_{41}Co_9Mn_{31.5}Ga_{18.5}$. Takahashi proposed a spin fluctuation theory of itinerant electron magnetism [44, 45]. The induced magnetization M is written as the formula of,

$$\left(\frac{M}{M_S}\right)^4 = 1.20\times10^6 \frac{T_C^2}{T_A^3 p_S^4}\cdot\frac{H}{M} \tag{2}$$

where, $M_S = N_0\mu_B p_S$ is a spontaneous magnetization in a ground state. N_0 is a molecular number. $p_S = g_S$, where g is the Landé g-factor and S is a spin angular momentum. T_A is the spin fluctuation parameter in k-space (momentum space). Nishihara et al. measured the magnetization of Ni and Ni_2MnGa precisely [55]. Direct proportionality was observed in the M^4 vs H/M plot at the Curie temperature for Ni. The critical index δ (defined as $H \propto M^{\delta}$) for Ni and Ni_2MnGa is 4.73 and 4.77, respectively. The critical index δ for Fe, CoS_2 and ferromagnetic Heusler alloys, Co_2VGa is 4.6, 5.2 and 4.93, respectively ([45] and references there in).

In most cases, the critical temperature dependence was determined using the Arrott plot. The analysis is based on the implicit assumption that the linearity is always satisfied. Takahashi suggested that the Arrott plot is not applicable in much itinerant d-electron ferromagnets and the revision is necessary in the itinerant electron magnetism [45].

Figure 11 shows the magnetization process of $Ni_{41}Co_9Mn_{31.5}Ga_{18.5}$ around the T_C^M. The horizontal axis is the external magnetic fields. As for the ferromagnetic materials, the diamagnetic effect should be concerned. The effective field H_{eff} is written as the formula of,

$$\mu_0 H_{eff} = \mu_0 H - \mu_0 NM \tag{3}$$

where H is the external magnetic fields, M is the measured magnetization value, and N is a diamagnetic factor. As for this sample, $N = 0.11$.

Eq. (2) can be written as the formula of,

$$H_{eff} = DM^{\delta} \tag{4}$$

and $\delta = 5$, and D is the constant value. From Eq. (4), δ was demanded using such an expression as below [56].

http://dx.doi.org/10.5772/64375

$$\frac{H_{eff}}{H_{eff\,\max}} = \frac{DM^{\delta}}{DM^{\delta}{}_{\max}} = \left(\frac{M}{M_{\max}}\right)^{\delta} \tag{5}$$

where $H_{\text{eff max}}$ is the maximum value of the effective magnetic fields, and $M_{\max}$ is the maximum value of the measured magnetization. δ can be demanded when a logarithm of the statement are taken, as the formula of, Eq. (5).

Figure 12 shows the logarithm plot of Eq. (5). The gradient of the X-Y plots indicate the critical index δ. **Table 3** shows the index δ and the standard deviation of δ around $T_C^M = 263$ K. Between 262 and 264 K, the error of δ is small. These results indicate that the critical index δ is 5.2(+-, plusminus sign) 0.2.

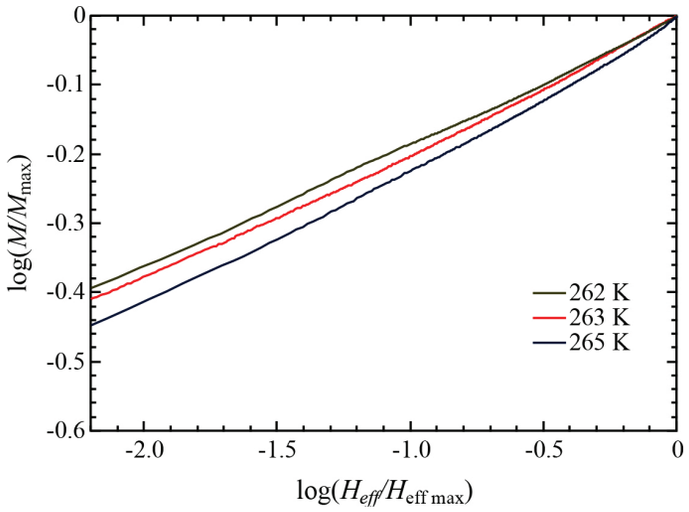

Figure 12. Logarithmic plot of $Ni_{41}Co_9Mn_{31.5}Ga_{18.5}$.

Figure 13 shows the M^4 vs H_{eff}/M plot of $Ni_{41}Co_9Mn_{31.5}Ga_{18.5}$ at $T_C^M = 263$ K. The M^4 vs H_{eff}/M plot crossed the coordinate axis at the Curie temperature in the martensite phase, T_C^M, and the plot indicates a good linear relation behavior around the T_C^M. The result was in agreement with the theory of Takahashi, concerning itinerant electron magnetism [21, 22]. From the M^4 vs H/M plot, the spin fluctuation temperature T_A can be obtained. The obtained T_A was 7.03×10^2 K and which was much smaller than Ni (1.76×10^4 K).

Table 4 indicates the values of p_s, T_C, and T_A estimated from magnetization measurements by means of Eq. (1). MnSi and URhGe are the compounds, which indicate small magnetic moment. The smallness of the moment p_s is due to the spin polarization. UGe_2 also indicate small magnetic moment compared to the full moment of U 5f electron, 3.6 μ_B/U. This is due to the large magnetic anisotropy, due to the spin polarization band [58–60]. The magnetic anisotropy energy is estimated as 6.17 meV = 107 T [58]. T_A is the spin fluctuation temperature, and it reflects width of the quasiparticle at the Fermi surface. Supposing that T_A is large, narrow quasi-fermion (electron) band is formed at the Fermi level and the correlations between quasi fermions are strong. The Zommerfeld coefficient γ also indicates the strength of the correlations

of the fermions (electrons). The γ of URhGe and UGe_2 are 163 and 110 mJ mol^{-1} K^{-2}, respectively. The γ of normal metals, Cu, Ni is around 1 mJ mol^{-1} K^{-2}. Therefore, the γ is two orders larger than that of normal metals. Supposing that γ is large, the narrow quasi-fermion (electron) band is formed at the Fermi level. The density of states of the band is large, which indicates the correlations of the electrons are large in U compounds. As for $Ni_{41}Co_9Mn_{31.5}Ga_{18.5}$, the T_A is 7.03×10^2 K, 6.45×10^2 K for $Ni_{52.5}Mn_{24.5}Ga_{23}$, and 4.93×10^2 K for Ni_2MnGa. These values are comparable to that of UGe_2 (4.93×10^2 K), This result indicates that the correlations of the electrons are strong in $Ni_{41}Co_9Mn_{31.5}Ga_{18.5}$, $Ni_{52.5}Mn_{24.5}Ga_{23}$, and Ni_2MnGa.

T (K)	Critical index δ	Standard deviation (%)
258	5.80	0.950
260	5.77	0.208
262	5.42	0.169
263	5.25	0.119
264	4.95	0.187
265	4.60	0.210

Table 3. The critical index δ and the standard deviation of δ around $T_C^M = 263$ K.

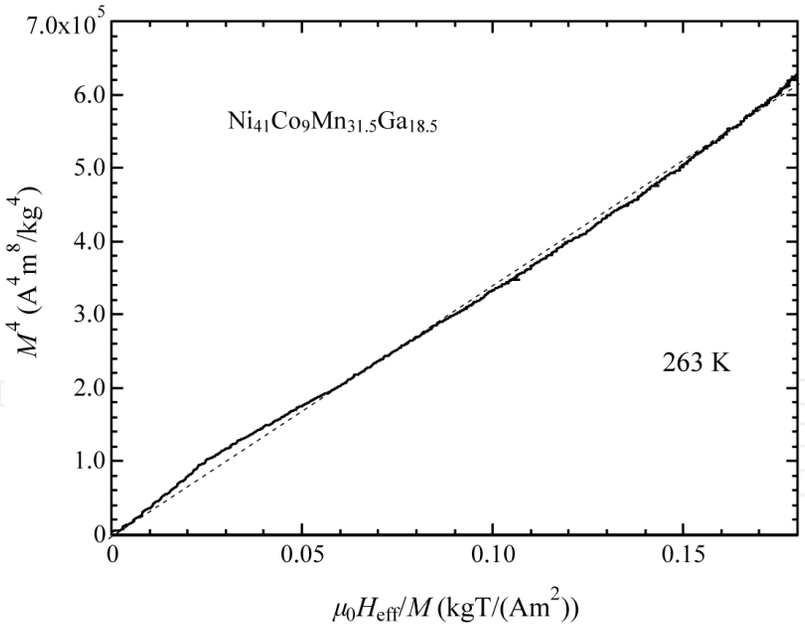

Figure 13. M^4 vs H_{eff}/M plot of $Ni_{41}Co_9Mn_{31.5}Ga_{18.5}$ at 263 K. Dotted line is the extrapolated line.

The value p_s of $Ni_{41}Co_9Mn_{31.5}Ga_{18.5}$, suggested in **Table 4**, is smaller than that of Ni_2MnGa. The small value of p_s has been observed at $Ni_{1.65}Co_{0.28}Mn_{1.31}Ga_{0.62}In_{0.67}$ [14]. The p_s of this alloy was 1.61 μ_B/f.u. at 5 T in ferromagnetic martensite phase. *M-H* curve shows metamagnetic transition at 42 and at 60 T, the magnetic moment reached to 5.0 μ_B/f.u. Karamad et al. point

http://dx.doi.org/10.5772/64375

to the Jahn-Teller effect as a source of the tetragonal distortion of the crystal structure of these alloys. However, they also suggested that the external magnetic field of 60 T seems to be high enough to suppress the Jahn-Teller distortion of crystal lattice of $Ni_{1.65}Co_{0.28}Mn_{1.31}Ga_{0.62}In_{0.67}$. Further experimental and theoretical investigations are needed to clarify this problem.

Compound	p_s (μ_B/f.u.)	T_C (K)	T_A (K)	Reference
Ni	0.6	623	1.76×10^4	[55]
MnSi	0.4	30	2.18×10^3	[45]
Co_2CrGa	3.01	488	1.0×10^4	[44]
Ni_2MnGa	4.5	363 (T_C^A)	4.63×10^2	[55]
$Ni_{52.5}Mn_{24.5}Ga_{23}$	3.75	350 (T_C^M)	6.45×10^2	[6, 57]
URhGe	0.32	9.6	8.56×10^2	[45]
UGe_2	1.44	53.5	4.93×10^2	[45]
$Ni_{41}Co_9Mn_{31.5}Ga_{18.5}$	1.74	263 (T_C^M)	7.03×10^2	This work

Table 4. Experimentally estimated values of p_s, T_C, and T_A from magnetization measurements.

4. Conclusions

We studied about the magnetocaloric properties of $Ni_{41}Co_9Mn_{31.5}Ga_{18.5}$ by means of differential scanning calorimetry (DSC) measurements. Magnetocalorimetric measurements and magnetization measurements of $Ni_{41}Co_9Mn_{31.5}Ga_{18.5}$ polycrystalline ferromagnetic shape memory alloy (FSMA) were performed across the T_R, at atmospheric pressure. When heating from the martensite phase, a steep increase in the thermal expansion due to the reverse martensite transition at T_R was observed by the thermal expansion measurements. These transition temperatures decreased gradually with increasing magnetic field. The field dependence of the reverse martensite transition temperature, $dT_R/d(\mu_0 H)$, is -7.0 K/T around zero fields. From the DSC measurements in zero fields, the value of the latent heat λ was obtained as 2.6 kJ/kg, and in magnetic fields, the value was not changed. The entropy change ΔS was -7.0 J/(kgK) in zero fields and gradually increases with increasing magnetic fields. The relative cooling power (RCP) was 104 J/kg at 2.0 T, which was comparable with in-doped $Ni_{41}Co_9Mn_{32}Ga_{16}In_2$ alloy [47].

In order to investigate the itinerant electron magnetic properties of $Ni_{41}Co_9Mn_{31.5}Ga_{18.5}$, we performed the magnetization measurements by means of the pulsed magnetic fields. The M^4 vs H/M plot crossed the coordinate axis at the Curie temperature in the martensite phase, T_{CM}, and the plot indicates a good linear relation behavior around the T_{CM}. The result was in agreement with the theory of Takahashi, concerning itinerant electron magnetism [44, 45]. From the M^4 vs H/M plot, the spin fluctuation temperature T_A can be obtained. The obtained

T_A was 7.03×10^2 K and which was smaller than Ni (1.76×10^4 K). The value was comparable to that of UGe_2 (4.93×10^2 K), which is famous for the strongly correlated heavy fermion ferromagnet [58].

Acknowledgements

The authors thank to Dr. M. Mori for helping SEM microscope experiment. DSC measurements in steady magnetic fields were performed at High Field Laboratory for Superconducting Materials, Institute for Materials Research, Tohoku University, Japan.

Author details

Takuo Sakon[1*], Takuya Kitaoka[1], Kazuki Tanaka[1], Keisuke Nakagawa[1], Hiroyuki Nojiri[2], Yoshiya Adachi[3] and Takeshi Kanomata[4]

*Address all correspondence to: sakon@rins.ryukoku.ac.jp

1 Department of Mechanical and System Engineering, Faculty of Science and Technology, Ryukoku University, Otsu, Shiga, Japan

2 Institute for Materials Research, Tohoku University, Sendai, Miyagi, Japan

3 Graduated School of Science and Engineering, Yamagata University, Yonezawa, Yamagata, Japan

4 Research Institute for Engineering and Technology, Tohoku Gakuin University, Tagajo, Miyagi, Japan

References

[1] K. Ullakko, J. K. Huang, C. Kantner, R. C. O'Handley and V. V. Kokorin, Large magnetic-field-induced strains in Ni_2MnGa single crystals. Appl. Phys. Lett. 69 (1996) 1966.

[2] P. J. Webster, K. R. A. Ziebeck, S. L. Town and M. S. Peak, Magnetic order and phase transformation in Ni_2MnGa. Philos. Mag. B. 49 (1984) 295.

[3] P. J. Brown, J. Crangle, T. Kanomata, M. Matsumoto, K-. U. Neumann, B. Ouladdiaf and K. R. A. Ziebeck, The crystal structure and phase transitions of the magnetic shape memory compound Ni_2MnGa. J. Phys. Condens. Matter. 14 (2002) 10159.

[4] J. Pons, R. Santamarta, V. A. Chernenko and E. Cesari, Long-period martensitic structures of Ni-Mn-Ga alloys studied by high-resolution transmission electron microscopy. J. Appl. Phys. 97 (2005) 083516.

[5] R. Ranjan, S. Banik, S. R. Barman, U. Kumar, P. K. Mukhopadhyay and D. Pandey, Powder X-ray diffraction study of the thermoelastic martensitic transition in $Ni_2Mn_{1.05}Ga_{0.95}$. Phys. Rev. B. 74 (2006) 224443.

[6] T. Sakon, K. Otsuka, J. Matsubayashi, Y. Watanabe, H. Nishihara, K. Sasaki, S. Yamashita, R. Y. Umetsu, H. Nojiri and T. Kanomata, Magnetic properties of the ferromagnetic shape memory alloy $Ni_{50+x}Mn_{27-x}Ga_{23}$ in magnetic fields. Materials 7 (2014) 3715.

[7] Y. Sutou, Y. Imano, N. Koeda, T. Omori, R. Kainuma, K. Ishida and K. Oikawa, Magnetic and martensitic transformations of NiMnX (X=In,Sn,Sb) ferromagnetic shape memory alloys. Appl. Phys. Lett. 85 (2004) 4358.

[8] K. Oikawa, W. Ito, Y. Imano, Y. Sutou, R. Kainuma, K. Ishida, S. Okamoto, O. Kitakami and T Kanomata, Effect of magnetic field on martensitic transition of $Ni_{46}Mn_{41}In_{13}$ Heusler alloy. Appl. Phys. Lett. 88 (2006) 122507.

[9] R. Y. Umetsu, R. Kainuma, Y. Amako, Y. Taniguchi, T. Kanomata, K. Fukushima, A. Fujita, K. Oikawa and K. Ishida, Mössbauer study on martensite phase in $Ni_{50}Mn_{36.5}{}^{57}Fe_{0.5}Sn_{13}$ metamagnetic shape memory alloy. Appl. Phys. Lett. 93 (2008) 042509.

[10] V. V. Khovaylo, T. Kanomata, T. Tanaka, M. Nakashima, Y. Amako, R. Kainuma, R. Y. Umetsu, H. Morito and H. Miki, Magnetic properties of $Ni_{50}Mn_{34.8}In_{15.2}$ probed by Mössbauer spectroscopy. Phys. Rev. B 80 (2009) 144409.

[11] R. Kainuma, Y. Imano, W. Ito, Y. Sutou. H. Morino, S. Okamoto, O. Kitakami, K. Oikawa, A. Fujita, T. Kanomata and K. Ishida, Magnetic-field-induced shape recovery by reverse phase transformation. Nature 439 (2006) 957.

[12] F. Albertini, S. Fabbrici, A. Paoluzi, J. Kamarad, Z. Arnold, L. Righi, M. Solzi, G. Porcari, C. Pernechele, D. Serrate and P. Algarabel, Reverse magnetostructural transitions by Co and In doping NiMnGa alloys: Structural, magnetic, and magnetoelastic properties mater. Sci. Forum 684 (2011) 151.

[13] C. Seguí, E. Cesari and P. Lázpita, Magnetic properties of martensite in metamagnetic Ni–Co–Mn–Ga alloys. J. Phys. D: Appl. Phys. 49 (2016) 165007.

[14] J. Kamarád, J. Kaštil, Y. Skourski, F. Albertini, S. Fabbrici and Z. Arnold, Magneto-structural transitions induced at 1.2 K in Ni_2MnGa-based Heusler alloys by high magnetic field up to 60 T. Mater. Res. Express 1 (2014) 016109.

[15] C. Seguí, Effects of the interplay between atomic and magnetic order on the properties of metamagnetic Ni-Co-Mn-Ga shape memory alloys. J. Appl. Phys. 115 (2014) 113903.

[16] P. Entel, M. E. Gruner, D. Comtesse, V. V. Sokolovskiy and V. D. Buchelnikov, Interacting magnetic cluster-spin glasses and strain glasses in Ni–Mn based Heusler structured intermetallics, Phys. Stat. Sol. B 251 (2014) 2135.

[17] J. Kamarád, S. Fabbrici, J. Kasštil, F. Albertini, Z. Arnold and L. Righi, Pressure dependence of magneto-structural properties of Co-doped off stoichiometric Ni_2MnGa alloys. EPJ Web Conf. 40 (2013) 11002.

[18] J. Kasštil, J. Kamarád, K. Knížek, Z. Arnold and P. Javorský, Peculiar magnetic properties of Er conditioned $Ni_{43}Co_7Mn_{31}Ga_{19}$ at ambient and hydrostatic pressures. J. Alloys Compd. 565 (2013) 134.

[19] G. Porcari S. Fabbrici, C. Pernechele, F. Albertini, M. Buzzi, A. Paoluzi, J. Kamarad, Z. Arnold and M. Solzi, Reverse magnetostructural transformation and adiabatic temperature change in Co- and In-substituted Ni-Mn-Ga alloys. Phys. Rev. B. 85 (2012) 024414.

[20] C. Segui and E. Cesari, Composition and atomic order effects on the structural and magnetic transformations in ferromagnetic Ni–Co–Mn–Ga shape memory alloys. J. Appl. Phys. 111 (2012) 043914.

[21] T. Kanomata, S. Nunoki, K. Endo, M. Kataoka, H. Nishihara, V. V. Khovaylo, R. Y. Umetsu, T. Shishido, M. Nagasako, R. Kainuma and K. R. A. Ziebeck, Phase diagram of the ferromagnetic shape memory alloys $Ni_2MnGa_{1-x}Co_x$. Phys. Rev. B. 85 (2012) 134421.

[22] Y. Wang, C. Huang, J. Gao, S. Yang, X. Ding, X. Song and X. Ren, Evidence for ferromagnetic strain glass in Ni-Co-Mn-Ga Heusler alloy system. Appl. Phys. Lett. 101 (2012) 101913.

[23] S. K. Ayila, R. Machavarapu and S. Vummethala, Site preference of magnetic atoms in Ni–Mn–Ga–M (M = Co, Fe) ferromagnetic shape memory alloys. Phys. Stat. Sol. B 249 (2012) 620.

[24] S. Fabbrici, J. Kamarad, Z. Arnold, F. Casoli, A. Paoluzi, F. Bolzoni, R. Cabassi, M. Solzi, G. Porcari, C. Pernechele and F. Albertini, From direct to inverse giant magnetocaloric effect in Co-doped NiMnGa multifunctional alloys. Acta Mater. 59 (2011) 412.

[25] P. O. Castillo-Villa, D. E. Soto-Parra, J. A. Matutes-Aquino, R. A. Ochoa-Gamboa, A. Planes, L. Mañosa, D. González-Alonso, M. Stipcich, R. Romero, D. Ríos-Jara and H. Flores-Zúñiga, Caloric effects induced by magnetic and mechanical fields in a $Ni_{50}Mn_{25-x}Ga_{25}Co_x$ magnetic shape memory alloy. Phys. Rev. B. 83 (2011) 174109.

[26] J. Bai, J. M. Raulot, Y. Zhang, C. Esling, X. Zhao and L. Zuo, The effects of alloying element Co on Ni–Mn–Ga ferromagnetic shape memory alloys from first-principles calculations. Appl. Phys. Lett. 98 (2011) 164103.

[27] D. E. Soto-Para, X. Moya, L. Mañosa, A. Planes, H. Flores- Zúñiga, F. Alvarado-Hernández, R. A. Ochoa-Gamboa, J. A. Matutes-Aquino and D. Ríos-Jara, Fe and Co

selective substitution in Ni_2MnGa: effect of magnetism on relative phase stability. Philos. Mag. 90 (2010) 2771.

[28] X. Xu, W. Ito, R. Y. Umetsu, K. Koyama, R. Kainuma, K. Ishida, Kinetic Arrest of Martensitic Transformation in $Ni_{33.0}Co_{13.4}Mn_{39.7}Ga_{13.9}$ Metamagnetic Shape Memory Alloy. Mater. Trans. 51 (2010) 469.

[29] B. M. Wang, P. Ren, Y. Liu and L. Wang, Enhanced magnetoresistance through magnetic-field-induced phase transition in Ni_2MnGa co-doped with Co and Mn. J. Magn. Magn. Mater. 322 (2010) 715.

[30] S. Yan, J. Pu, B. Chi and L. Jian, Estimation of driving force for martensitic transformation in $(Ni_{52.5}Mn_{23.5}Ga_{24})_{100-x}Co_x$ alloys. J. Alloys Compd. 507 (2010) 331.

[31] S. Fabbrici, F. Albertini, A. Paoluzi, F. Bolzoni, R. Cabassi, M. Solzi, L. Righi and G. Calestani, Reverse magnetostructural transformation in Co-doped NiMnGa multifunctional alloys. Appl. Phys. Lett. 95 (2009) 022508.

[32] Y. Ma, S. Yang, Y. Liu and X. Liu, The ductility and shape-memory properties of Ni–Mn–Co–Ga high-temperature shape-memory alloys. Acta Mater. 57 (2009) 3232.

[33] L. Ma, H. W. Zhang, S. Y. Yu, Z. Y. Zhu, J. L. Chen, G. H. Wu, H. Y. Liu, J. P. Qu and Y. X. Li, Magnetic-field-induced martensitic transformation in MnNiGa:Co alloys. Appl. Phys. Lett. 92 (2008) 032509.

[34] V. Sánchez-Alarcos, J. I. Pérez-Landazábal, V. Recarte, C. Gómez-Polo and J. A. Rodríguez-Velamazán, Correlation between composition and phase transformation temperatures in Ni–Mn–Ga–Co ferromagnetic shape memory alloys. Acta Mater. 56 (2008) 5370.

[35] D. Y. Cong, S. Wang, Y. D. Wang, Y. Ren, L. Zuo and C. Esling, Martensitic and magnetic transformation in Ni–Mn–Ga–Co ferromagnetic shape memory alloys. Mater. Sci. Eng. A 473 (2008) 213–218.

[36] X. Q. Chen, X. Lu, D. Y. Wang and Z. X. Qin, The effect of Co-doping on martensitic transformation temperatures in Ni–Mn–Ga Heusler alloys. Smart Mater. Struct. 17 (2008) 065030.

[37] P. Entel, M. E. Gruner, W. A. Adeagbo and A. T. Zayak, Magnetic-field-induced changes in magnetic shape memory alloys. Mater. Sci. Eng. A 481–482 (2008) 258–261.

[38] Y. Ma, S. Yang, C. Wang and X. Liu, Tensile characteristics and shape memory effect of $Ni_{56}Mn_{21}Co_4Ga_{19}$ high-temperature shape memory alloy. Scr. Mater. 58 (2008) 918–921.

[39] S. Y. Yu, Z. X. Cao, L. Ma, G. D. Liu, J. L. Chen, G. H. Wu, B. Zhang and X. X. Zhang, Realization of magnetic field-induced reversible martensitic transformation in NiCoMnGa alloys. Appl. Phys. Lett. 91 (2007) 102507.

[40] I. Glavatskyy, N. Glavatska, O. Söderberg, S.-P. Hannula and J.-U. Hoffmann, Transformation temperatures and magnetoplasticity of Ni–Mn–Ga alloyed with Si, In, Co or Fe. Scr. Mater. 54 (2006) 1891–1895.

[41] T. Sakon, Y. Adachi, R. Y. Umetsu, H. Nojiri, H. Nishihara and T. Kanomata, Crystallography and Magnetic Field-Induced Strain by Co Doping NiCoMnGa Heusler Alloy, TMS2013 Supplemental Proceeding, pp. 967–974, 2013, Wiley, USA.

[42] C. Seguí and E. Cesari, Contributions to the transformation entropy change and influencing factors in metamagnetic Ni-Co-Mn-Ga shape memory alloys. Entropy 16 (2014) 5560.

[43] A, E. Clark, J. D. Verhoeven, O. D. McMasters and E. D. Gibson, Magnetostriction in twinned [112] crystals of $Tb_{0.27}Dy_{0.73}Fe_2$. IEEE Trans. Magn. Mag. 22 (1986) 973.

[44] Y. Takahashi, Quantum spin fluctuation theory of the magnetic equation of state of weak itinerant-electron ferromagnets. J. Phys.: Condens. Matter. 13 (2001) 6323–6358.

[45] Y. Takahashi, *Spin Fluctuation Theory of Itinerant Electron Magnetism;* Springer-Verlag: Berlin/Heidelberg, Germany, 2013.

[46] T. Sakon, K. Sasaki, D. Numakura, M. Abe, H. Nojiri, Y. Adachi and T. Kanomata, Magnetic field-induced transition in Co-doped $Ni_{41}Co_9Mn_{31.5}Ga_{18.5}$ Heusler Alloy. Mater. Trans. 54 (2013) 9–13.

[47] S. Fabbrici, G. Porcari, F. Cugini, M. Solzi, J. Kamarad, Z. Arnold, R. Cabassi and F. Albertini, Co and In doped Ni-Mn-Ga magnetic shape memory alloys: a thorough structural, magnetic and magnetocaloric study. Entropy 16 (2014) 2204–2222.

[48] F. -X. Hu, B-G. Shen, J. -O. Sun and G. -H. Wu, Large magnetic entropy change in a Heusler alloy $Ni_{52.6}Mn_{23.1}Ga_{24.3}$ single crystal. Phys. Rev. B 64 (2001) 132412.

[49] M. Pasquale, C. P. Sasso, L. H. Lewis, L. Giudici, T. Lograsso and D. Schlagel, Magnetostructural transition and magnetocaloric effect in $Ni_{55}Mn_{20}Ga_{25}$ single crystals. Phys. Rev. B. 72 (2005) 094435.

[50] A. K. Nayak, K. G. Suresh and A. K. Nigam, Magnetic, electrical, and magnetothermal properties in Ni–Co–Mn–Sb Heusler alloys. J. Appl. Phys. 107 (2010) 09A927.

[51] A. K. Pathak, I. Dubenko, J. C. Mabon, S. Stadler and N. Ali, The effect of partial substitution of In by *X* = Si, Ge and Al on the crystal structure, magnetic properties and resistivity of $Ni_{50}Mn_{35}In_{15}$ Heusler alloys. J. Phys. D: Appl. Phys. 42 (2009) 045004.

[52] D. Bourgault, J. Tillier, P. Courtois, D. Maillard and X. Chaud, Large inverse magnetocaloric effect in $Ni_{45}Co_5Mn_{37.5}In_{12.5}$ single crystal above 300 K. Appl. Phys. Lett. 96 (2010) 132501.

[53] G. Porcari, F. Cugini, S. Fabbrici, C. Pernechele, F. Albertini, M. Buzzi, M. Mangia and M. Solzi, Convergence of direct and indirect methods in the magnetocaloric study of

first order transformations: The case of Ni-Co-Mn-Ga Heusler alloys. Phys. Rev. B. 86 (2012) 104432.

[54] V. Sokolovskiy, A. Gruünebohm, V. Buchelnikov and P. Entel, *Ab Initio* and Monte Carlo approaches for the magnetocaloric effect in Co- and In-doped Ni-Mn-Ga Heusler alloys. Entropy 16 (2014) 4992.

[55] H. Nishihara, K. Komiyama, I. Oguro, T. Kanomata and V. Chernenko, Magnetization processes near the Curie temperatures of the itinerant ferromagnets. Ni_2MnGa and pure nickel. J. Alloys. Compd. 442 (2007) 191.

[56] M. Seeger, S. N. Kaul, H. Kronmüller and R. Reisser, Asymptotic critical behavior of Ni. Phys. Rev. B. 51 (1995) 12585.

[57] In Ref. [6] (Sakon et al., Materials 2014), The calculated result of T_A was incorrect. From the experimental results of the magnetic moment and the gradient of M^4 vs. H/M, which are shown in Ref. [6], the calculated spin fluctuation parameter T_A is 645 K.

[58] T. Sakon, S. Saito, K. Koyama, S. Awaji, I. Sato, T. Nojima, K. Watanabe and N. K. Sato, Experimental investigation of giant magnetocrystalline anisotropy of UGe_2. Phys. Scr. 75 (2007) 546–550.

[59] V. G. Storchak, J. H. Brewer, D. G. Eshchenko, P. W. Mengyan, O. E. Parfenov and D. Sokolov, Spin-polaron band in the ferromagnetic heavy-fermion superconductor UGe_2. J. Phys.: Conf. Ser. 551 (2014) 012016.

[60] F. Hardy, D. Aoki, C. Meingast, P. Schweiss, P. Burger, H. V. Löhneysen and J. Flouquet, Transverse and longitudinal magnetic-field responses in the Ising ferromagnets URhGe, UCoGe, and UGe_2. Phys. Rev. B. 83 (2011) 195107.

IntechOpen